

Investigation of Inhibition Effects in Acrylate/Epoxy Hybrid Systems Using Raman Confocal Microscopy

*Ying Cai and Julie L. P. Jessop
Chemical & Biochemical Engineering, University of Iowa
Iowa City, IA 52246*

Abstract

The hybrid monomer 3,4-epoxy-cyclohexyl-methyl methacrylate, which contains both acrylate double-bond and epoxide ring moieties, was initiated by free-radical and/or cationic photopolymerization to produce a thin coating. Conversion and chemical composition at the surface and different depths were obtained by Raman confocal microscopy. The effect of formulation and atmosphere upon surface quality and chemical composition was investigated. Conversion depth profiles approached bulk values, and cross-linking at epoxide sites decreased sensitivity to atmosphere and improved film-forming properties.

Introduction

Photopolymerization has drawn great attention due to its advantages of room-temperature reactions, fast curing speeds, energy efficiency, easy reaction control, and low volatile organic contents. Applications in which photopolymerization is used include films and coatings, inks, adhesives, fiber optics, and dentistry.^{1,2} The two main types of initiation mechanisms used commercially are free radical and cationic. Hybrid photopolymerizations, which contain two types of functional groups, have arisen in recent years. For example, free-radical and cationic photopolymerization systems such as acrylate/epoxides³⁻⁶ and acrylate/vinyl ether^{5,7,8} hybrid systems have been reported. This study focuses on hybrid monomer systems bearing both acrylate and epoxides functionalities, which have tremendous promise for solving the oxygen inhibition and moisture problems that plague free-radical and cationic polymerizations, respectively. Acrylates, which undergo free-radical polymerization, exhibit high reaction rates and offer a large selection of monomers and initiators; while epoxides, which undergo cationic ring-opening photopolymerization, do not suffer from oxygen inhibition and exhibit low toxicity and shrinkage. These so-called hybrid photopolymerizations combine the advantages of these two reaction pathways and offer less shrinkage, lower sensitivity to both oxygen and moisture, and improved adhesion and flexibility. However, there is an important need for fundamental knowledge about the reactions (and interactions) in these systems in order to optimize the development of these systems for commercial applications.

Inhibition Effects

Free-radical polymerization is known to be inhibited by molecular oxygen, which can quench the excited triplet state of photoinitiator molecules and scavenge the initiator and polymer radicals.^{1,2,9} Much research has focused on the mechanism of oxygen inhibition towards free-radically initiated polymerization and how to prevent this effect, to enable the application, and to improve product quality. Common approaches to combating oxygen inhibition include: expensive inerting equipments, waxes, shielding films that can be used to prevent oxygen from entering the system; higher concentration of free-radical photoinitiator or high intensity irradiation sources to produce a larger number of radicals to consume the oxygen faster and allow the polymer chains to grow;^{1,2} and the addition of other chemical additives such as amines to capture the oxygen.^{11,12} However, these methods also increase the manufacturing cost and sometimes result in further problems with the products. For example, high concentrations of photoinitiator will decrease the light penetration to the bottom of the coating, resulting in lower conversion, which can lead to poor adhesion to the substrate.

Cationic photopolymerization has become more prevalent since the synthesis of effective photoinitiators, such as diaryliodonium and triarylsulfonium salts, were synthesized.^{1,13,14} It has become a possible alternative to traditional free-radical photopolymerization systems due to its oxygen insensitivity. However, moisture effects upon the cationic photopolymerization have to be considered due to the multiple roles that water serves in the polymerizing system and the impacts on the resulting polymers. For instance, water acts as a hydrogen donor in the photoinitiation process to generate the superacid, which initiates the polymerization. At the same time, the initiator can be deactivated by hydrolysis of the super acid in the water-rich environment, thus inhibiting the reaction.¹⁵ Moreover, water is an effective chain-transfer agent, leading to higher final conversion and shorter chain length or lower cross-linking density in the resulting polymer, which has great impact on the physical properties.¹⁶

Raman Spectroscopy

To obtain good surface and physical properties for coatings and films, a high degree of conversion is needed. For a free-radical photopolymerization system reacting in the air, polymerization will not start until the dissolved oxygen concentration has been reduced to as low as 10^{-5} M;¹⁷ thus, an induction period will be present. As the reaction proceeds, more radicals are consumed as oxygen continues to diffuse into the system. Under this condition, thin films are unable to cure and thicker films will retain a tacky surface with a higher conversion at the bottom. If the reaction could be monitored in real-time and depth profiles of the conversion through the coatings and films could be obtained, then the reaction kinetics, effects of oxygen and water, conversion of functional groups, and formulation could be correlated. This information would aid the optimization of formulations and develop a better understanding of how oxygen and water affect the different layers of the coatings. It would also provide insight on how the conversion at different depths affects the surface quality, physical properties and adhesion to substrate of the final product.

In-situ investigations of photopolymerizations have been carried out by using differential

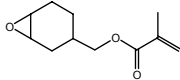
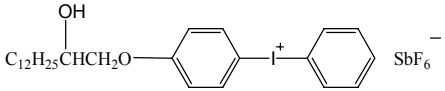
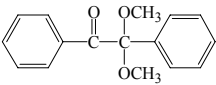
scanning calorimetry (DSC)^{4,6} and real-time infrared (RTIR)^{3,6,7} and Raman¹⁸ spectroscopy. In this study, real-time Raman spectroscopy was used to monitor the photopolymerization of hybrid monomers first, and then the cured coating samples were investigated by Raman confocal microscopy, a non-destructive method, to obtain profiles of functional group conversions at various sample depths. The Raman scattering technique is based upon the rotational and vibrational transitions in molecules and is particularly well suited for the detection of chemical bonds and their changes during reaction. The combination of microscopy and Raman spectroscopy greatly improves the spatial resolution, and the depth resolution can be further improved by introducing a confocal arrangement. In the latter arrangement, the chemical composition at a given depth can be obtained using a pinhole in the back image plane of the microscope objective to filter out Raman effects above and below the sampling plane. Thus, an optical slice of the sample can be obtained without physically touching the sample. Raman microscopy can identify areas ten times smaller than can be determined by FTIR microscopy, providing better resolution for surface and depth investigations. It is also able to investigate the depth up to several tens of microns, which is much greater than with attenuated total reflectance (ATR) FTIR spectroscopy, which is only applicable to (couple microns).¹⁹ This technique has been used for depth-profiling different multilayer and photo-curing polymer coatings and films.²⁰ Models have been developed to relate the experimental location with the true focusing point location to further improve depth resolution and spatial accuracy, which worsen with increasing depth.²¹⁻²³

Materials and Methods

Materials

The basic photopolymerization system under investigation in this research consists of the monomer and photoinitiator. The resins that have been chosen for this study are based on (meth)acrylates and epoxides. These resins can be UV-cured by using either a cationic or free-radical photoinitiator alone or a hybrid free-radical/cationic photoinitiator system. The photoinitiators chosen for this study are a diaryl iodonium cationic photoinitiator and an α -cleavable free-radical photoinitiator based on the benzoyl chromophore. All materials discussed in this proceeding are shown in Table 1.

Table 1. Monomers and photoinitiators used in this research.

Function	Chemical Name	Acronym	Structure
Hybrid monomer	3,4-epoxy-cyclohexyl methyl methacrylate	METHB	
Cationic photoinitiator	diaryliodonium hexafluoroantimonate	DAI	
Free-radical photoinitiator	2,2-dimethoxy-2-phenylacetophenone	DMPA	

Methods

A 785-nm near-infrared laser was used to induce the Raman scattering effect. Real-time data were collected using the Mark II holographic fiber-coupled stretch probehead (Kaiser Optical Systems, Inc.) attached to the HoloLab 5000R modular research Raman spectrograph (Kaiser Optical Systems, Inc). A 10x non-contact sampling objective with 0.8-cm working distance was used. Samples were cured at room temperature in 1-mm ID quartz capillary tubes using the Acticure[®] Ultraviolet/Visible Spot Cure System (EFOS). The exposure time for spectra was 500 ms.

A Leica DMLP optical microscope with confocal optics attached to the HoloLab 5000R modular research Raman spectrograph was used to obtain spectra of the monomer and depth profiles of photopolymer coatings. A combination of 785-nm single-mode excitation fiber and 15- μm collection fiber was used for the microscope studies. A 10x objective (with numerical aperture equal to 0.25 and a 5.8-mm working distance) was used to study the monomer. The exposure time for monomer spectra was 5 s. Coatings for the depth-profiling study were produced by spreading one droplet of monomer mixture on a quartz slide and illuminating for 45 minutes at ambient conditions with the Acticure[®] system using a light intensity of 100 mW/cm². Raman spectra of the coatings were taken starting from the sample surface to the bottommost layer with 120-s exposure time using a 100x objective (with numerical aperture equal to 0.9 and a 0.27-mm working distance). Compared to the real-time Raman spectroscopic technique, which uses a higher laser intensity (~220 mW) and investigates a larger (bulk) sample volume, this Raman confocal microscopy technique uses ~9-mW laser intensity over a spot size of 1.5 μm with a depth resolution of 3 μm . Since the most interested depth in this study is near surface (0-15 μm) where the spatial accuracy is still relatively reliable, we did not use the models for further depth determination.

Results and Discussion

These studies investigated the reaction kinetics of METHB and the conversion of the two functional groups in METHB at various sample depths using Raman confocal microscopy. The Raman spectrum of METHB is shown in Figure 1. The reactive bands representing the methacrylate C=C double bond and epoxide ring, which are used to calculate conversion, are located at 1640 and 790 cm^{-1} , respectively. The methacrylate COO functional group, which has a constant peak at 605 cm^{-1} , was selected as the internal reference band.

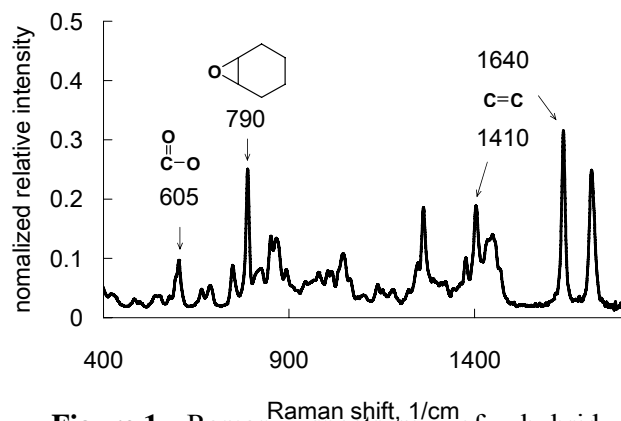


Figure 1. Raman spectrum of hybrid monomer METHB.

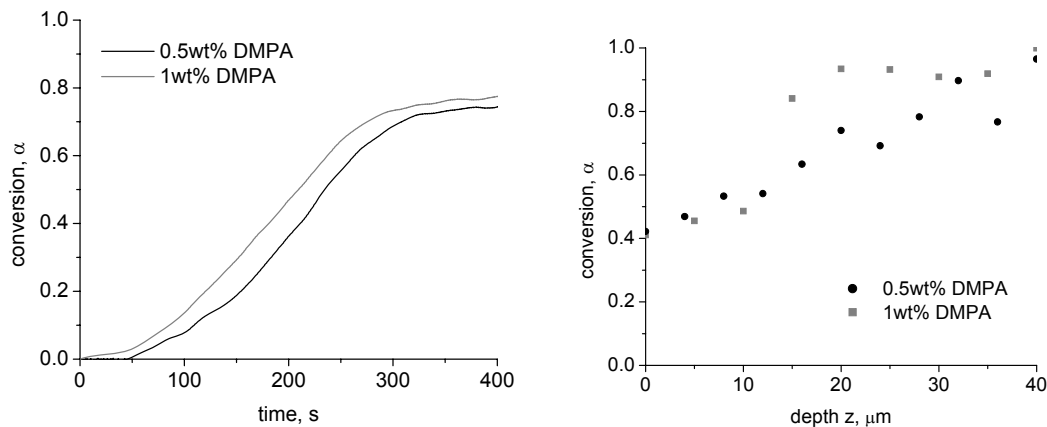


Figure 2. Real-time reaction profiles (left) and depth profiles (right) of the acrylate C=C double bond conversion in METHB formulations with 0.5wt% DMPA and 1wt% DMPA at room temperature and light intensity of 100 mW/cm².

Effect of Oxygen Inhibition

Free-radical initiator only. Coatings with METHB and the free-radical initiator DMPA were studied using Raman spectroscopy. The real-time experimental results are shown in Figure 2 (left). A higher concentration of DMPA resulted in higher reaction rate, higher C=C double bond conversion and shorter induction period. The resulting photopolymer coatings were then studied by Raman confocal microscopy (Figure 2, right). Both coatings showed low conversion (only 40-50%) at the surface ($z < 15 \mu\text{m}$), which matched the physical condition of the coatings (*i.e.*, tacky surfaces), because oxygen continues to diffuse into the coating during cure and consumes the free-radical active centers. As viscosity increases during polymerization, it becomes more difficult for oxygen to penetrate throughout the coating, facilitating higher final conversion values at deeper levels. Thus, the conversion in single free-radical initiator hybrid systems increases as the depth increases. In the 0.5wt%-DMPA formulation, the conversion gradually increases with depth until it reaches a plateau value around $z = 15 \mu\text{m}$; however, the 1wt%-DMPA formulation exhibited a sudden increase of conversion from 50% at $z = 10 \mu\text{m}$ to ~85% at $z = 15 \mu\text{m}$. This behavior is due to the higher concentration of initiator, which produces a greater number of active centers and retards the diffusion of oxygen. The conversion did not show a dependence on the depth after 15 μm , at which point it agreed well with the ultimate conversion measured in the real-time Raman studies.

Dual-initiator system. Coatings with METHB and both DMPA and DAI were also studied with Raman spectroscopy. This system exhibits cross-linking since the polymer chains can be connected via the epoxide or acrylate reactive bonds. Thus, the ultimate conversions of C=C double bond and epoxide ring measured in real-time are about 70% and 10%, respectively (see Figure 3). The acrylate bond conversion is less than that shown in Figure 2 (left) due to cross-linking in the polymer at the epoxide sites. Figure 3 shows four different combinations of the two photoinitiators. Formulations with higher concentrations of DMPA resulted in faster reaction rates and shorter induction periods for the C=C double bond compared with the single initiator systems. With the

same amount of DMPA, the systems with higher concentration of DAI have shorter induction periods but similar reaction rates after the reaction started. In these systems, radicals generated by the cationic initiator can consume some oxygen, thereby reducing the induction period; however, these radicals are not able to initiate the free-radical polymerization of the double bonds. No difference was shown for the epoxide ring conversion profiles among these four formulations. The epoxide ring opening reaction is much slower than the double bond reaction, and the mobility of the cationic reactive centers is restricted after the onset of cross-linking during polymerization.

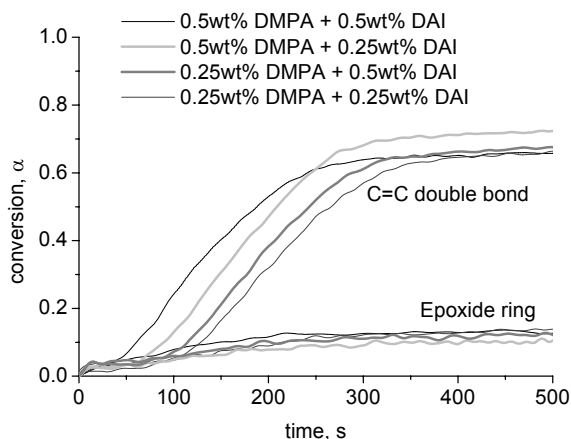


Figure 3. Real-time reaction profiles of the acrylate C=C double bond and epoxide-ring conversions in METHB formulations with different concentrations of DMPA and DAI photopolymerized at room temperature and light intensity of 100 mW/cm².

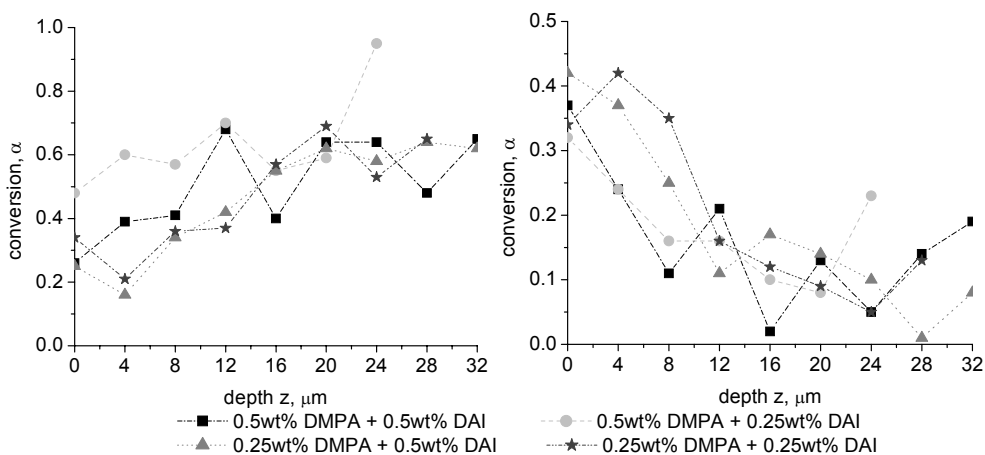


Figure 4. Depth profiles of C=C double bond (left) and epoxide-ring (right) conversions in METHB coatings with different concentrations of DMPA and DAI photopolymerized at ambient condition and light intensity of 100 mW/cm².

In the depth profiles of the polymer samples, the acrylate bond conversion at the surface increases 15-30% (see Figure 4, left) from 0 to 12 μm , while the conversion of the epoxide rings drops 25-35% over the same length scale (see Figure 4, right). In addition, the cross-linked hybrid polymers had non-tacky and smooth surfaces, even though the conversion of the acrylate bonds was not high. This surface hardness is attributable to the presence of the reacted epoxide rings. The coatings with higher concentrations of DMPA showed a higher conversion of C=C double bond and a lower conversion of epoxide ring at the surface. Compared with the conversion of C=C double bond for the system containing 0.5wt% DMPA, the conversion of the acrylate bonds in the two-initiator system was higher at a 12- μm depth. The reaction of epoxide rings effectively decreases oxygen diffusion from the air interface to the coating interior, facilitating increased conversion. At depths greater than 12 μm , the acrylate bond conversion of the two-initiator system is about 70% and is again comparable with real-time Raman results. As in the single free-radical initiator system, the depth-profile patterns of dual-initiator systems are similar: a gradual increase in conversion for lower concentrations of DMPA and step-function increase for higher concentrations.

Surface hardness testing of the photopolymer coatings. Finally, pencil hardness tests based on ASTM D33363 were performed on all four coatings (see Table 2). The formulations containing only free-radical initiator resulted in tacky surfaces due to oxygen inhibition. However, all formulations containing both free-radical and cationic initiators showed 6H gouge hardness. Differences arose in the scratch hardness results for different concentrations of the initiators. In general, higher concentrations of both initiators provided better surface quality and vice versa.

Table 2. Comparison of physical properties of the resulting photopolymer coatings.

	Initiator System	Pencil Hardness	
		Gouge	Scratch
Free-radical initiator only	0.5wt% DMPA	Tacky surface	
	1wt% DMPA		
Dual-initiator system	0.5wt% DMPA + 0.5wt% DAI	6H	5H
	0.5wt% DMPA + 0.25wt% DAI	6H	4H
	0.25wt% DMPA + 0.5wt% DAI	6H	4H
	0.25wt% DMPA + 0.25wt% DAI	6H	3H

Effect of Water Concentration

Free-radical initiator only. Coatings with METHB and the free-radical initiator DMPA were studied using real-time Raman spectroscopy. Increasing water concentration slows down the reaction rate of the C=C double bond (see Figure 5). It also results in a slight increase of the final conversion of the acrylate functional group due to the plasticizing effect of water.

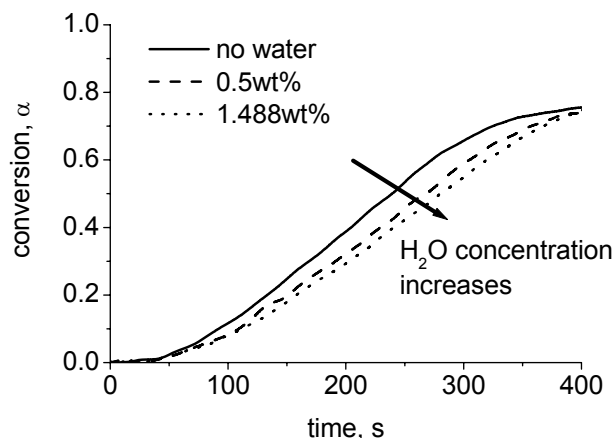


Figure 5. Real-time reaction profiles of the acrylate C=C double bond conversion of METHHB with 0.5wt% DMPA and increasing water concentration photopolymerized at room temperature and light intensity of 100 mW/cm².

Cationic initiator only. In cationic ring-opening polymerizations, water serves multiple functions: as a hydrogen donor, an inhibitor, and a chain-transfer agent. Figure 6 (left) shows the effect of increasing water concentration on the epoxide-ring reaction of METHHB initiated only by DAI. Increasing water concentration resulted in an extended induction period for this monomer. The water molecules react with the cationic end of the growing chain and result in hydroxyl end groups and a new cationic center, which is the so-called chain transfer reaction.^{15,16,24} Thus, the addition of water causes an increase in the rate of polymerization and ultimate conversion. Figure 6 (right) shows the depth profiles of three different formulations. The conversion throughout the polymer became more homogeneous with increasing water content. Similar to the results of the real-time experiments, higher average conversions of the epoxide ring were reached when water was added into the formulation.

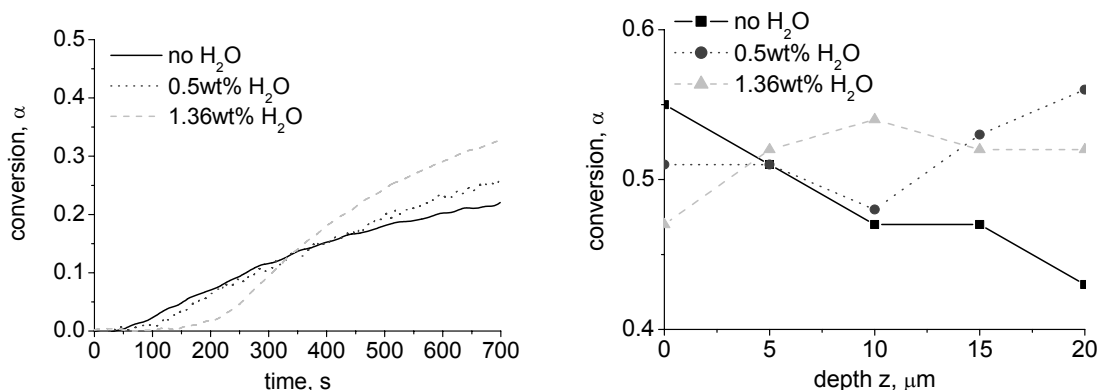


Figure 6. Real-time reaction profiles (left) and depth profiles (right) of the epoxide-ring conversion of METHHB with 0.5wt% DAI and increasing water concentration photopolymerized at room temperature and light intensity of 100 mW/cm².

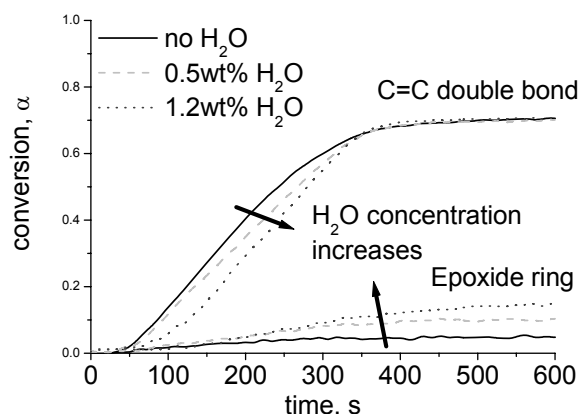


Figure 7. Real-time reaction profiles of the acrylate C=C double bond and epoxide-ring conversions in METHHB formulations with 0.5wt% DMPA and 0.5wt% DAI and increasing water concentration photopolymerized at room temperature and light intensity of 100 mW/cm².

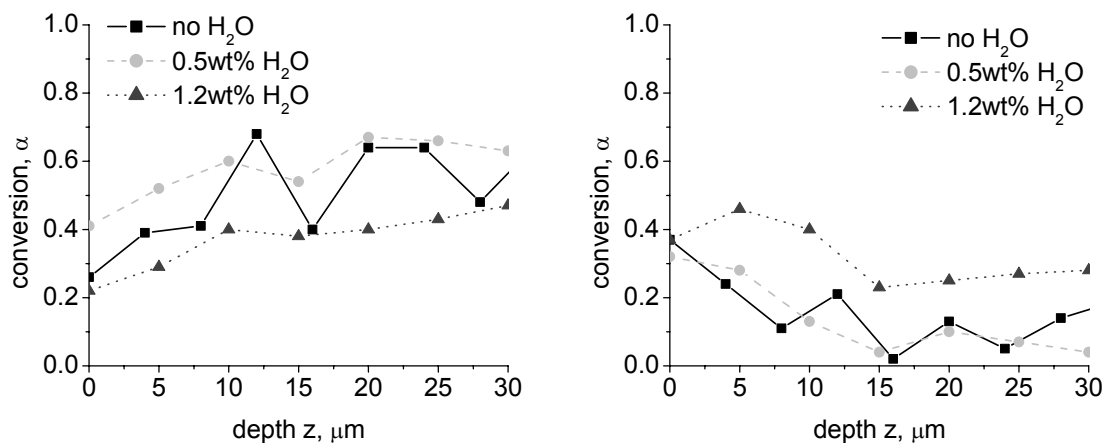


Figure 8. Depth profiles of the acrylate C=C double bond (left) and epoxide-ring (right) conversions of METHHB with 0.5wt% DMPA and 0.5wt% DAI and increasing water concentration photopolymerized at room temperature and light intensity of 100 mW/cm².

Dual-initiator system. Coatings with METHHB, free-radical initiator DMPA, and the cationic initiator DAI were studied with Raman spectroscopy. Figure 7 shows the hybrid systems cured by a dual free-radical/cationic initiation scheme with increasing amounts of water added. Similar to the free-radical initiator only systems, the reaction rate of C=C double bond decreased. The ultimate conversion of the epoxide ring significantly increased as the water concentration increased. However, there was no dependence of the cationic induction period on the water concentration compared with the previous cationic initiator only systems. This is caused by lower sensitivity to moisture in the dual-initiator system, in which decomposition of the cationic initiator is promoted by the free-radicals present.²⁵ The depth profiles of both functional groups (see Figure 8) of water-added formulations followed a similar trend as of the formulation without additional water. However, with addition of large amounts of water, (i.e., 1.2wt%), a drastic decrease of C=C double

bond conversion at all the depths was observed, while the conversion of the epoxide-ring was much higher than those systems with little or no water added.

Conclusions

This research has demonstrated that real-time Raman spectroscopy is effective for simultaneous reaction monitoring of the C=C double bond and epoxide ring in these hybrid systems. The reaction rate and conversion were both affected by the choice of initiation system. Homopolymers result from a single-initiator system, cross-linked polymers from a dual-initiator system. Quantitative conversion differences of the C=C double bond and the epoxide ring were measured at the surface and the bottom for coatings cured in ambient conditions by Raman confocal microscopy without destroying the samples. The conversion depth-profile pattern showed a strong dependence upon the initiation system as well. The cross-linking network resulting from the dual-initiator system reduced oxygen inhibition problems and offered improved surface properties. The effects of water concentration upon the reaction mechanism and depth profile in hybrid monomers cured by different initiation schemes were also studied. Generally, an increase in water concentration resulted in an extended induction period and increased rate of polymerization and ultimate conversion. Further investigation and interpolation of these systems are ongoing, and a better understanding will be obtained by correlating the reaction mechanism, chemical composition and physical properties.

Acknowledgements

This material is based upon work supported by the National Science Foundation under Grant No. 0133133 and the University of Iowa. We would like to acknowledge Daicel and Sartomer for providing the materials used in this study.

References

1. J.P. Fouassier, Photoinitiation, *Photopolymerization, and Photocuring: Fundamentals and Applications*, Hanser Publishers, New York, 1995.
2. J. V. Koleske, *Radiation Curing of Coatings*, ASTM International, West Conshohocken, 2002.
3. C. Decker, T. Nguyen Thi Viet, D. Decker, E. Weber-Koehl, *Polymer* 42, 5531 (2001).
4. J.D. Oxman, D.W. Jacobs, M.C. Trom, V. Sipani, B. Ficek, A.B. Scranton, *J. Polym. Sci., Part A: Polym. Chem.*, 43, 1747 (2005).
5. J.D. Cho and J.W. Hong, *J of Applied Polymer Science*, 93, 1473 (2004).
6. K.M. Dean and W.D. Cook, *Polymer International*, 53, 1305 (2004).
7. Y. Lin, and J.W. Stansbury, *Polymer*, 44, 4781 (2003).
8. K. Dean, W.D. Cook, M.D. Zipper, P. Burchill, *Polymer*, 42, 1345 (2001).
9. G. Odian, *Principles of Polymerization, 3rd Ed.*, John Wiley & Sons, Inc., New York, 1991.
10. C. Decker and A.D. Jenkins, *Macromolecules*, 18, 1241 (1985).

11. J. P. Fouassier, and J. F. Rabek, ed., *Radiation Curing in Polymer Science and Technology—Volume III: Polymerisation Mechanisms*, Elsevier Applied Science, New York, 1993.
12. C.W. Miller, C.E. Hoyle, S. Jonsson, C. Nason, T.Y. Lee, W.F. Kuang, K. Viswanathan, *Photoinitiated Polymerization, ACS Symposium*, 847, 2 (2003).
13. J.V. Crivello, *Adv. Polym. Sci.*, 62, 1 (1984).
14. Y. Yagci and T. Endo, *Adv. Polym. Sci.* 127, 59 (1997).
15. A. Hartwig, A. Harder, A. Lühring, H. Schröder, *Eur Polym J*, 37, 1449 (2001).
16. A. Hartwig, *International Journal of Adhesion & Adhesives*, 22, 409 (2002).
17. C. Decker and A. Jenkin, *Macromolecules*, 18, 1241 (1985).
18. E.W. Nelson, and A.B. Scranton, *Journal of Polymer Science: Part A: Polymer Chemistry*, 34, 403 (1996).
19. T. Scherzer, *Vibrational Spectroscopy*, 29, 139 (2002).
20. W. Schrof, E. Bech, G. Etzrodt, H. Hintze-Brüning, U. Meisenburg, R. Schwalm, J. Warming, *Progress in Organic Coatings*, 43, 1 (2001).
21. N.J. Overall, *Applied Spectroscopy*, 54, 1515 (2000).
22. L. Baia, K. Gigant, U. Posset, G. Schottner, W. Kiefer, J. Popp, *Applied Spectroscopy*, 56, 536 (2002).
23. S.J. Spells, H. Reinecke, J. Sacristan, J. Yarwood, C. Mijangos, *Macromol. Symp.* 203, 147 (2003).
24. Y. Yagci and W. Schnabel, *Die Angewandte Makromolekulare Chemie*, 270, 38 (1999).
25. M. Degimenci, Y. Hepuzer, Y. Yagci, *J Appl Polym Sci*, 85, 2389 (2002).